Available online at www.sciencedirect.com
SCIENCE DIRECT®
Journal of Electron Spectroscopy and Related Phenomena 150 (2006) 228–234
JOURNAL OF ELECTRON SPECTROSCOPY and Related Phenomena
www.elsevier.com/locate/elspec

Force spectroscopy of bonds that form between a *Staphylococcus* bacterium and silica or polystyrene substrates

Ruchirej Yongsunthon, Steven K. Lower*

The Ohio State University, 275 Mendenhall Laboratory, 125 South Oval Mall, Columbus, OH 43210, USA

Available online 19 September 2005

Abstract

Inter- and intra-molecular forces are the driving forces responsible for the creation of an interface between a microorganism and a naturally occurring mineral or man-made material. We have used atomic force microscopy to directly measure forces between a *Staphylococcus aureus* bacterium and each of two materials (silica and polystyrene) in an electrolyte solution. Force "spectra" were collected by placing a glass or polystyrene bead (~10 μm diameter) in contact with a living cell and then pulling the two surfaces apart. An attractive, adhesion force was observed in approximately 40 and 50% of the measurements for silica and polystyrene, respectively. The strength of the adhesion bond was 38 ± 4 pN (10^{-12} N) and 52 ± 9 pN for glass and polystyrene, respectively. The origin of the attractive interaction appears to be non-specific (e.g., van der Waals force) although a small number (2–3%) of force spectra contained distinct sawtooth like profiles indicative of a protein bond between *S. aureus* and glass or polystyrene.

Keywords: Adhesion; Atomic force microscopy; Bacteria; Bond; Force; Polystyrene; Protein; Silica; *Staphylococcus aureus*; van der Waals

1. Introduction

On Earth, most (>97%) of the millions of different species of prokaryotes live in contact with one or more of the 3000 different mineral species that occur in the soil and subsurface environments [1–3]. The creation of man-made materials, such as plastics and alloys has provided microorganisms with other niches in the environment. Arguably this makes the microbe–mineral or, more generally, the microbe–material interface the most significant interface in nature.

The structure and reactivity of this interface can be described in terms of a number of parameters including: the macromolecules (e.g., proteins, lipids, polysaccharides) on a microorganism, the surface properties (e.g., surface charge density, topography) of a material, and the composition of the aqueous solution between the material and microbe. Regardless of the specifics of these parameters, at its very essence each microbe–material interface is defined by and, in fact, created by fundamental inter- and intra-molecular forces between a cell and an inorganic or organic surface.

Over the last few years, atomic force microscopy (AFM) has become the instrument of choice for probing forces between surfaces. Fig. 1 provides a diagram and brief description of our AFM experimental setup. We and our colleagues have used AFM to measure forces that a bacterial cell experiences as it approaches a material surface, as well as the force necessary to decouple bonds that may form once a cell makes contact with a material surface (e.g., see refs. [4–9]). The latter measurement is often termed "force spectroscopy", because the AFM force-data profiles (also known as force curves) have the appearance of spectra-data. However, AFM actually measures forces by monitoring the physical deflection of a mechanical, force-sensing cantilever rather than observing electromagnetic spectra per se.

This manuscript is intended to provide the reader with an introduction to AFM force spectra measurements between bacteria and other surfaces immersed in aqueous solution. We will present force–distance profiles describing the relationship between a Gram-positive *Staphylococcus aureus* and two different materials, silica and polystyrene, that are commonly found in the environment. These data will be interpreted in terms of the maximum force necessary to separate a cell from a material surface, and the total amount of potential energy encapsulated within the cell–material interface. The measured force–distance profiles will also be compared to a theoretical force–extension model to identify putative macromolecules (e.g., proteins)

* Corresponding author.
E-mail address: lower.9@osu.edu (S.K. Lower).

0368-2048/$ – see front matter © 2005 Elsevier B.V. All rights reserved.
doi:10.1016/j.elspec.2005.06.012

that may form a physical bond between a cell and another surface.

2. Methods and materials

2.1. Preparation of materials for AFM measurements

Materials used in these experiments included both silica and polystyrene beads (~10 μm in diameter; from Duke Scientific and Polysciences, Inc.). A single glass or polystyrene bead was attached to the end of a silicon-nitride cantilever with epoxy resin (see Fig. 1 for reference). These colloid-probes were used in an AFM to probe living bacteria cells.

Prior to their use, glass beads were cleaned in a mixture of sulfuric acid and hydrogen peroxide [10] to remove any proprietary coating. These glass beads were then rinsed ten times in ultrapure water (MilliQ water). The surface roughness of the glass bead was determined by using AFM in "image mode" to collect a topographic image of the silica surface. The root mean squared (rms) roughness was determined to be 1.8 nm over a 1 μm^2 area. The range of vertical relief on the glass bead was 27 nm.

Polystyrene beads were cleaned by rinsing three times in ultrapure water. AFM was also used to collect a topographic image of the surface of the polystyrene beads. The rms roughness was determined to be 4.5 nm over a 1 μm^2 area with a vertical range of 35 nm.

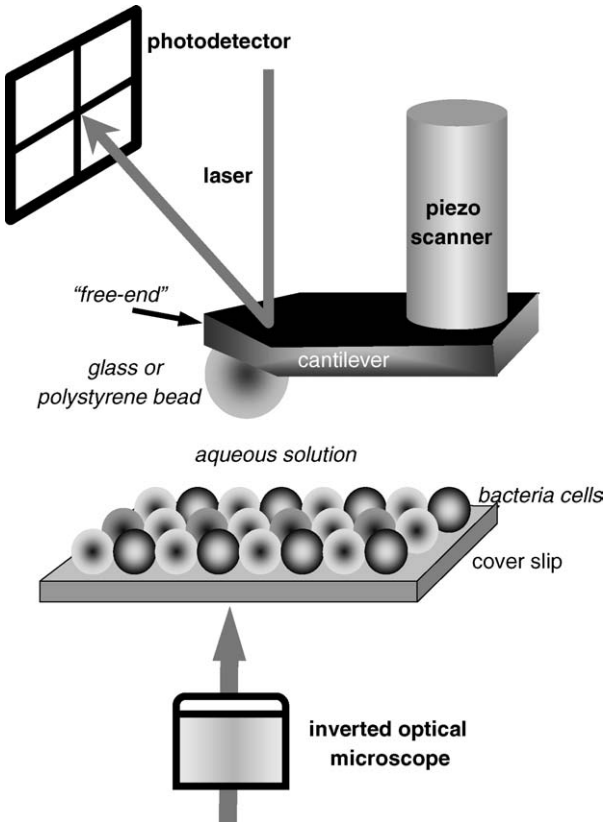

Fig. 1. Schematic diagram showing the key components of an atomic force microscope (AFM), which, in this case, has been mounted on an inverted optical microscope. The cantilever and sample are within a fluid cell (not shown) containing aqueous solution. Force measurements are made by recording the deflection of a sensor (i.e., cantilever) in response to attractive or repulsive forces between a bead, mounted on the "free end" of the cantilever, and a bacterium on a cover slip. A piezoelectric scanner is used to translate the "fixed end" of the cantilever. In so doing, the bead indexes towards, makes contact with, and retracts from a cell. Deflection of the "free end" of the cantilever is monitored by reflecting a laser off the top of the cantilever and into a split segment photodiode. The data presented in this paper are the force "spectra" or retraction curves collected when a bead is pulled away from a bacterium. This figure is not to scale.

2.2. Preparation of bacteria cells for AFM measurements

Bacteria used in these experiments included a wild-type strain of *S. aureus* kindly provided by A. Peschel. *Staphylococcus* is a Gram-positive, facultative aerobe that typically occurs as pairs or clusters of cocci cells [11]. Individual cells are approximately 1 μm in diameter. Bacteria were grown to exponential phase in tryptic soy media, and harvested by centrifugation at 5000 × *g* for 3 min. Harvested cells were washed three times in 50 mL of sterile 0.1 M NaCl, blotted onto a glass cover slip with a sterile pipette tip, rinsed after 5–10 min to remove loose cells, and used in an AFM.

Fig. 2 shows *S. aureus* cells on a cover slip that was used in the AFM to collect force spectra. The image shown in Fig. 2 was collected with a sharp tip using the AFM in "image mode". For force measurements (described below), a colloid-probe was vertically translated towards and away from a living cell on a cover slip, which was immersed in aqueous solution.

2.3. Atomic force microscopy in water

A commercial AFM (Veeco/Digital Instruments; Bioscope AFM) was used to collect force measurements in a circumneu-

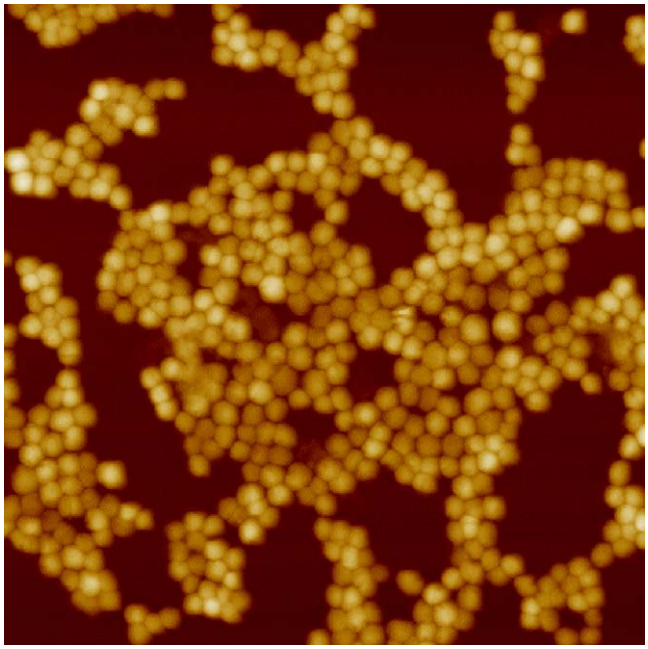

Fig. 2. Atomic force micrograph of a wild-type strain of *Staphylococcus aureus* on a cover slip. This image is 25 μm on a side. A sharp cantilever tip, as opposed to the colloid bead probe (shown in Fig. 1) was used to image these bacteria cells.

tral, electrolyte solution containing 0.1 M sodium chloride. In the "force mode" set up the x and y piezoelectric scanners are disabled so that movements are made only in the z (i.e., vertical) direction.

Cells were located on a cover slip by using transmitted light and a 100X/1.45 N.A. objective (Zeiss α-Plan-Fluar) on an inverted optical microscope attached to the AFM (see Fig. 1 for reference). A colloid-probe was positioned directly over a monolayer patch of cells. The cantilever was translated towards a bacterium on a cover slip using the z piezoelectric scanner. Once contact was established, the cantilever was pushed to a maximum loading force (i.e., force of the bead on the cell wall) of 1–4 nN. Finally, the cantilever was pulled away from the bacterium's surface.

A diode laser was used to monitor the deflection of the cantilever in response to attractive or repulsive forces between a bacterium and the bead on the end of the cantilever. The raw-data were collected as the output of the photodiode detector (which is directly proportional to the deflection of the cantilever) as a function of the displacement of the z piezoelectric scanner (which controls the position of the bead relative to the bacteria sample). Subsequent to AFM measurements, cell viability was confirmed by observing the bacteria divide in a small quantify of broth which was placed onto the bacteria-coated cover slip.

A sample approach–retraction curve is shown in Fig. 3. These data begin as the bead and *Staphylococcus*-coated cover slip are far apart resulting in the initial deflection-free portion of the approach curve (i.e., horizontal line). The bead is then brought into contact with a cell and subsequently pushed against the cell surface causing an upward deflection of the cantilever. This region of contact is sometimes referred to as the "region of constant compliance". The movement of the piezo is then reversed such that the bead is pulled away from the cell resulting in the retraction curve. Retraction begins as a linear relaxation of the cantilever deflection followed by, in some cases, a downward deflection due to adhesion forces between the bead and bacterium. Finally, the cantilever snaps back to its deflection-free position after adhesion forces are overcome. An entire approach–retraction cycle typically takes less than 1 s. It is the retraction curve that is often referred to as force spectra.

Raw data, plotted as so-called "voltage–displacement" curves (Fig. 3A), can be converted into "force–distance" curves (Fig. 3B) according to a well-established protocol [12,13]. Voltage data were converted into force data using the spring constant ($nN\,nm^{-1}$) of the cantilever and the optical lever sensitivity, which is a measure of the cantilever flexion per voltage of photodiode output ($nm\,V^{-1}$). For these measurements, the cantilever spring constant was determined to be $0.02\,N\,m^{-1}$ using the hydrodynamic drag method of Craig and Neto [14]. The optical lever sensitivity was determined from the inverse slope of the region of constant compliance, where the tip is in hard contact with the surface, thus forcing the cantilever to flex in direct response to z-piezo displacement. It is worth noting that this procedure for determining the optical lever sensitivity is valid only for situations in which the cantilever is the most

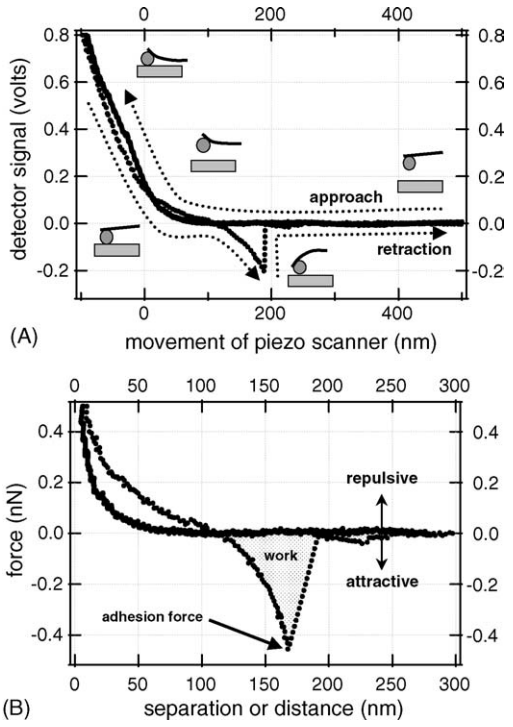

Fig. 3. Schematic diagrams of (A) voltage–displacement and (B) force–distance curves. When the cantilever or more specifically, the bead on the cantilever, and sample are far apart they exhibit no interaction (region of no contact or zero force). As the cantilever approaches the sample (from right to left), intermolecular forces between the bead and sample cause the cantilever to deflect upwards in this case due to repulsive forces. Eventually, the bead on the cantilever makes contact with the sample and their movement becomes coupled (region of constant compliance). The bead is then retracted from the sample (left to right) until the cantilever and sample return to their original positions thereby completing one cycle. The detector signal (V) is converted into force (nN) using the optical lever sensitivity ($nm\,V^{-1}$) and the cantilever spring constant (in $nN\,nm^{-1}$). The displacement of the piezoelectric scanner is converted into separation by correcting for the deflection of the cantilever and by selecting a point of contact (i.e., origin of the x axis). By convention repulsive forces are positive and attractive forces are negative. Hysteresis, shown here, may occur upon retraction due to the formation of an attractive, adhesion force (see label). The work or energy associated with a retraction curve can be described by integrating force with respect to distance (see shaded region).

compliant (i.e., flexible) component of the system. If another component (e.g., a cell) is more compliant than the cantilever then there will not be a 1:1 correlation between the flexure of the "free end" of the cantilever and the movement of the z piezoelectric scanner. This will be discussed again in Section 3 below.

Displacement of the z-piezo was converted into distance or separation values by correcting the movement of the piezoelectric scanner by the cantilever's deflection, and selecting the origin of the separation axis (i.e., distance of zero) as the "beginning" or "end" of the region of constant compliance (see Fig. 3). The resulting force–distance curves were analyzed with SPIP (Image Metrology) and Igor Pro (WaveMetrics) software. Only retractions curves are discussed herein as these are typically referred to as force spectroscopy in the literature.

3. Results and discussion

3.1. Force spectra between Staphylococcus and glass or polystyrene in aqueous solution

Either a glass or polystyrene bead (∼10 μm diameter) was brought into contact with a *S. aureus* cell on a cover slip. The bead was then pulled from a cell while monitoring the force required to retract the cantilever a certain distance (i.e., retraction data or force spectra). This was repeated on 15–20 different cells from three different cultures of bacteria. Two different glass bead and two different polystyrene bead probes were used in these AFM experiments.

Fig. 3B shows one force profile obtained between *S. aureus* and a silica glass bead in 0.1 M NaCl. The approach curves for glass (and polystyrene) exhibited purely repulsive forces of interaction with *S. aureus*. However, ∼40% of the retraction curves exhibited an attractive, adhesion force with glass (e.g., see retraction curve in Fig. 3B). For polystyrene, ∼50% of the retraction curves revealed an adhesion event with *S. aureus*.

The inverted optical microscope (see Fig. 1) made it relatively easy to ensure that a silica (or polystyrene) bead made contact with a *Staphylococcus* cell. As a control we collected force measurements between a silica (or polystyrene) bead and a cell-free area of the glass cover slip used to support the bacteria (see Fig. 2). These control curves exhibited only repulsive forces in keeping with purely electrostatic forces between glass and either polystyrene or another glass surface (data not shown).

The raw force curves for the *Staphylococcus* bead measurements yielded values for the optical lever sensitivity (i.e., the slope of the region of constant compliance) that varied somewhat. In particular, the region of constant compliance for some curves could be defined by two lines of different slope. For example, in some measurements optical lever sensitivity values varied from ∼100 to ∼200 nm V^{-1}. Fig. 4 shows what happens when different values for the optical lever sensitivity are applied to the exact same "voltage–displacement" curve. Not only is the force axis significantly impacted but also the separation (or distance) axis.

Such differences in the optical lever sensitivities are not uncommon when soft materials such as cells are probed with an AFM. This is because the cell is more compliant than the cantilever, for small compressions. Therefore, the region of constant compliance, which provides the nm V^{-1} conversion factor (see Fig. 3), includes the combined effects of cantilever flexion and cell compression. In essence, the cantilever deflects less per unit of *z*-piezo movement as some of its deflection is absorbed by the cell. Therefore, this portion of the voltage–displacement curve will not accurately reflect cantilever response and will result in a smaller slope of the region of constant compliance (small V nm^{-1}) and a larger optical lever sensitivity (large nm V^{-1}).

Rather than using a particular curve's region of constant compliance to determine its optical lever sensitivity, we determined an average optical lever sensitivity on a rigid glass surface before and after force measurements with bacteria cells. A number of silicon nitride cantilevers, manufactured from the same wafer, were fitted with glass beads. These glass bead cantilevers were pressed against a hard glass surface in the same electrolyte solution used with the bacteria. In doing so, we ensured that the cantilever was the most compliant component of the system. The resulting optical lever sensitivity ranged from 130 to 135 nm V^{-1}. We used these values to determine force–distance curves (or force spectra) for the measurements shown herein.

It is worth noting that if the cantilever is pushed with sufficient force, the soft components of a surface will typically reach their limit of compression, after which the cantilever becomes the most compliant element in the system. Although these extreme regions of constant compliance more accurately indicate the cantilever response, the forces required often damage the cells and/or contaminate the colloid-probe with cell components. Potential contamination of the colloid-probes used in these experiments was evaluated by periodically measuring forces on a clean glass surface (data not shown).

Fig. 5 shows several force spectra observed when a glass or polystyrene substrate was retracted from an *S. aureus* bacterium in 0.1 M NaCl. The maximum adhesion force in individual spectra ranged from a few picoNewton to more than 0.5 nN. As

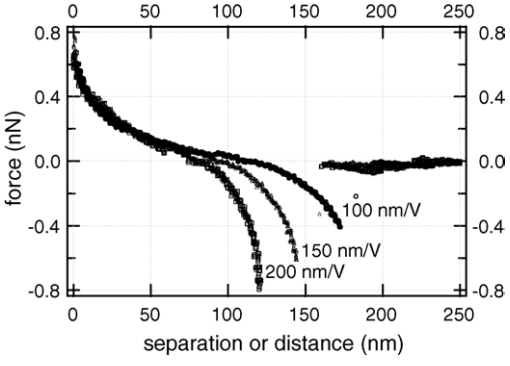

Fig. 4. Force–distance curves (i.e., force spectra) for a bead being pulled away from a *S. aureus* bacterium in 0.1 M NaCl solution. All three curves were generated from the same voltage–displacement data (i.e., raw data) by using different values for the optical lever sensitivity (see values in nm V^{-1} on each curve). As shown here, the optical lever sensitivity impacts not only the derived force values but also the separation distance.

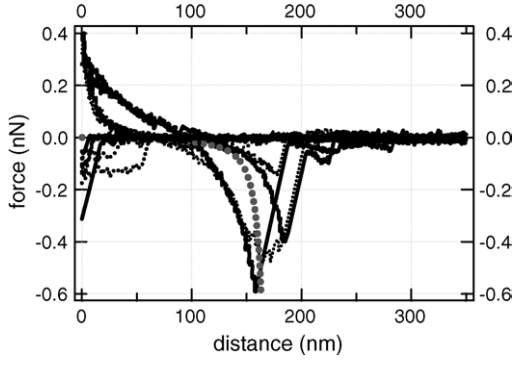

Fig. 5. Force–distance curves (i.e., force spectra) recorded when a silica or polystyrene bead was pulled from contact with a living *S. aureus* bacterium in saline solution. Most spectra show only "jump from contact features" (see region from 0 to 25 nm). Some profiles have a distinct "sawtooth" shape (see region from 100 to 200 nm). The worm-like chain model (Eq. (1)) was used to predict the force–extension relationship for a cell wall protein that formed a bond with the surface of a bead (dotted gray-colored curve).

noted above, only 40–50% of the retraction curves revealed an attractive interaction. For those retraction curves that showed an attractive force, most were unremarkable, exhibiting only a "jump from contact" feature (see retraction curves between 0 and 25 nm in Fig. 5). This occurs when the spring constant of the cantilever exceeds the actual force-gradient between the cell and glass (or polystyrene) causing the bead to decouple from the cell or "jump" from contact with the cell. Such features are consistent with non-specific, attractive interactions such as the van der Waals force. A few retraction curves (2–3%), particularly for polystyrene, exhibited a long-range attractive bond that displayed a "sawtooth" like profile (see retraction curves between 100 and 200 nm in Fig. 5).

3.2. Adhesion force and energy (or work) determinations

To compare force spectra for the two materials used in these experiments, we plotted histograms of the maximum adhesion force observed between *S. aureus* and a silica or polystyrene bead. The adhesion force was found to be larger for bacteria on polystyrene relative to glass (Fig. 6A).

One shortcoming of this approach is that the adhesion force represents but one datum point on a retraction curve. For bacterium–material interactions that are long range (tens to hundreds of nanometer) the entire force spectra can be embodied in a single energy or work value. This is accomplished by integrating force with respect to distance (see Fig. 3B) in spectra such as those shown in Fig. 5. Fig. 6B shows a histogram of the work or energy (in attoJoules) required to separate a *Staphylococcus* cell from silica or polystyrene. Like the adhesion forces (Fig. 6A), there was a significant difference for the work/energy values for glass versus polystyrene.

Because the beads used in these experiments were all the same size (radius ~5 μm), the difference in affinity between *S. aureus* and glass versus polystyrene is likely due to the different surface properties of these two materials. Table 1 presents values related

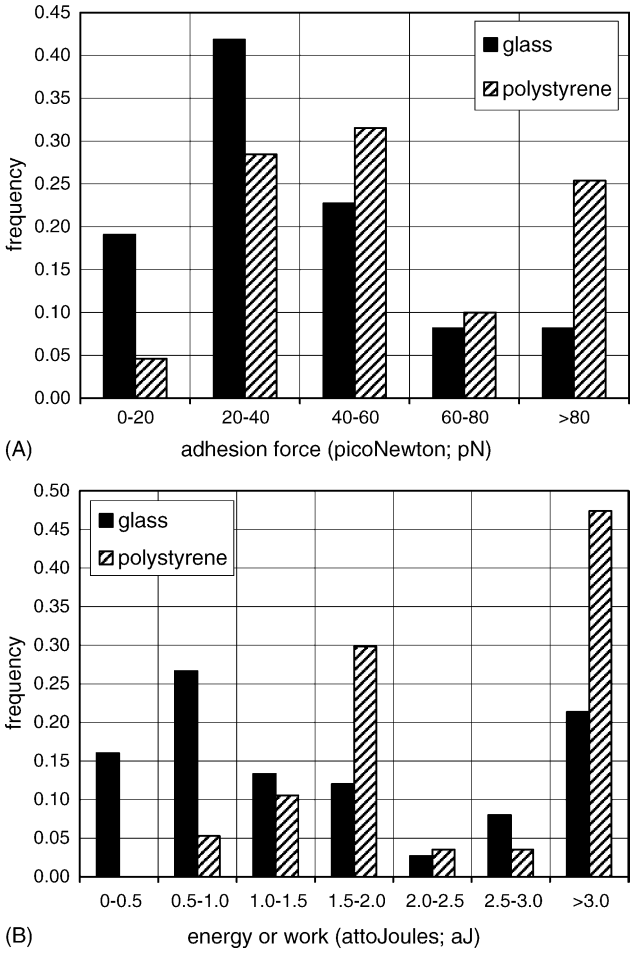

Fig. 6. Histograms describing the frequency for which a particular adhesion force or determination of work was observed in the force spectra. (A) For those retraction curves that exhibited adhesion, the average adhesion force for silica glass and polystyrene are 38 ± 4 pN (10^{-12} N) and 52 ± 9 pN, respectively. (B) Likewise, the average work/energy necessary to completely separate *S. aureus* from silica or polystyrene are 1.5 aJ (10^{-18} J) and 2.3 aJ, respectively. Retraction curves that did not display any attractive bond were not included in these histograms.

Table 1
Comparison of surface properties of silica and polystyrene

Surface potential (mV)	
Silica[a]	−21 to −35
Polystyrene[b]	−35 to −75
Contact angle (°)	
Silica[c]	0 to 5
Polystyrene[d]	82 to 96
Surface roughness (nm)	
Silica[e]	1.8 to 3
Polystyrene[f]	4.5

[a] From references [13,24,25] for circumneutral solutions composed of 0.1 M NaCl, KCl or KNO_3.
[b] From references [16,26,27] for circumneutral solutions composed of 0.1 M NaCl or KNO_3.
[c] From reference [28] for water.
[d] From reference [29] for ultrapure water and reference [28] for 0.01 M sodium phosphate solution.
[e] From reference [13] for measurement of peak-to-peak roughness of silica bead and rms analysis shown in this work.
[f] From rms analysis shown in this work.

to the surface charge, hydrophobicity and surface roughness of silica and polystyrene. For comparison, the surface potential for *Staphylococcus* cells is −2 to −10 mV and the contact angle of a buffer solution on a monolayer of *Staphylococcus* is 20–37° [15]. The surface roughness of a bacterium is difficult to measure because of the dynamic nature of macromolecules on a cell's surface. As a gross estimate, we measured a range of values from 40 to 80 nm for the rms roughness on a 1 μm^2 area of *Staphylococci* shown in Fig. 2.

The surface charge for both materials (Table 1) and the bacteria [15] are negative. Therefore, it seems unlikely that the overall surface charge can explain the observed attractive bonds in the force spectra. On the other hand, the surface roughness and, to a lesser extent, the hydrophobicity, seem to provide an explanation as to why a greater force/energy is observed between *S. aureus* and polystyrene relative to silica.

The rms roughness of the polystyrene bead is 1.5–2.5 times greater than that of the glass bead (see Table 1). This greater roughness is likely due to the surface structure of the polystyrene

bead, which consists of "hairs" or "brushes" of polymer that extend into solution ([16] and L. Luce, Polysciences Inc., personal communication, 2004). Greater surface roughness is expected to lead to a greater force of van der Waals attraction [17] and decreased electrostatic repulsion between particles of the same charge [18]. Hence, most of the attractive interactions between *S. aureus* and the two materials (see "jump from contact" features in Fig. 5) appear to be the result of non-specific interactions such as the van der Waals force.

3.3. Identification of macromolecules that form a bond

The previous discussion reveals that there is a clear distinction between the adhesion force/work of adhesion experienced by *S. aureus* on polystyrene versus silica glass. *S. aureus* has a stronger affinity for polystyrene presumably because of stronger non-specific forces. However, a limited number of the retraction curves between *S. aureus* and polystyrene show a unique "sawtooth" like feature (see Fig. 5). These are regions of the spectra where force increases non-linearly and then suddenly recoils back towards the line of zero force. Recently, we showed that such sawtooth features represent the physical decoupling of a protein that forms a specific bond between a bacterium and a substrate [19]. The origin of these sawteeth can be understood by comparing the retraction curves to theoretical models, which have been developed to describe force–extension relationships of polymers such as proteins.

One such model, called the worm-like chain theory, was developed to predict the entropic elasticity of linear polymers [20,21]. This model treats a polymer as a relatively stiff rod made of homogeneous elastic material (e.g., amino acids), and predicts the force (F) necessary to extend the polymer a given distance (x). The equation for the worm-like chain model is given as [20]:

$$F(x) = \left(\frac{k_B T}{p}\right)\left[0.25\left(1-\frac{x}{L}\right)^{-2} + \frac{x}{L} - 0.25\right] \quad (1)$$

where p is the persistence length (in m), L the contour length (in m), k_B the Boltzmann's constant (1.381×10^{-23} J K^{-1}) and T is the temperature (in K).

The persistence length (p) is a measure of the elasticity of a polymer or the distance over which a polymer retains "memory" of a given direction [22]. For proteins a persistence length of ~0.4 nm represents the distance between alpha carbons (C_α) in a polypeptide chain [23]. Selecting a contour length (L), or fully extended length, of 175 nm yields the curve plotted on Fig. 5. The shape of the worm-like chain model takes on a sawtooth like profile that is strikingly similar to the measured force spectra. Each of the observed sawteeth can be described by Eq. (1) by simply changing the contour and persistence lengths, to account for the size and stiffness, respectively, of a polypeptide chain forming a bond between the bacterium and material substrate. This suggests that proteins on the bacterium surface are occasionally able to form a specific bond between the cell and glass or polystyrene.

4. Conclusions

This manuscript provides quantitative data describing the force of attraction between a *S. aureus* bacterium and each of two materials (silica and polystyrene) in an electrolyte solution. This bacterium formed an attractive bond with either surface approximately 40–50% of the time. The strength of this bond was 38 ± 4 pN (10^{-12} N) and 52 ± 9 pN for glass and polystyrene, respectively. The origin of this bond was likely due to non-specific forces such as the van der Waals force. In some instances, the force spectra displayed a unique sawtooth signature. These spectra were compared to the worm-like chain model (Eq. (1)), which provides a theoretical description of the force necessary to extend a protein macromolecule. This comparison suggests that proteins on the cell wall of the bacterium occasionally (<3% of the time) formed a specific, physical bond with the material substrates.

Acknowledgements

Portions of this work were funded by the National Science Foundation and the Department of Energy. The authors would like to thank D. Baer for inviting us to submit this manuscript. This manuscript was improved by the helpful comments of two anonymous reviewers. S.K.L. acknowledges the support of J. Tak.

References

[1] R.V. Gaines, H.C.W. Skinner, E.E. Foord, B. Mason, A. Rosenzweig, Dana's New Mineralogy: The System of Mineralogy of James Dwight Dana and Edward Salisbury, John Wiley and Sons, New York, 1997.
[2] W.B. Whitman, D.C. Coleman, W.J. Wiebe, Proc. Natl. Acad. Sci. U.S.A. 95 (1998) 6578.
[3] V. Torsvik, L. Ovreas, T.F. Thingstad, Science 296 (2002) 1064.
[4] S.K. Lower, C.J. Tadanier, M.F. Hochella, Geochim. Cosmochim. Acta 64 (2000) 3133.
[5] S.K. Lower, M.F. Hochella, T.J. Beveridge, Science 292 (2001) 1360.
[6] S.K. Lower, C.J. Tadanier, M.F. Hochella, Geomicrobiol. J. 18 (2001) 63.
[7] S.K. Lower, M.F. Hochella Jr., J.F. Banfield, K. Rosso, Eos: Trans. Am. Geophys. Union 83 (2002) 53.
[8] T.A. Kendall, S.K. Lower, Adv. Agronomy 82 (2004) 1.
[9] S.K. Lower, Am. J. Sci., in press.
[10] Y.-S. Lo, N.D. Huefner, W.S. Chan, P. Dryden, B. Hagenhoff, T.P. Beebe Jr., Langmuir 15 (1999) 6522.
[11] M.T. Madigan, J.M. Martinko, J. Parker, Brock Biology of Microorganisms, Prentice Hall, Upper Saddle River, New Jersey, 2003.
[12] W.A. Ducker, T.J. Senden, R.M. Pashley, Nature 353 (1991) 239.
[13] W.A. Ducker, T.J. Senden, R.M. Pashley, Langmuir 8 (1992) 1831.
[14] V.S.J. Craig, C. Neto, Langmuir 17 (2001) 6018.
[15] J.L. Prince, R.B. Dickinson, Langmuir 19 (2003) 154.
[16] J.E. Seebergh, J.C. Berg, Colloids Surf. A 100 (1995) 139.
[17] K. Cooper, N. Ohler, A. Gupta, S. Beaudoin, J. Colloid Interface Sci. 222 (2000) 63.
[18] E.M.V. Hoek, S. Bhattacharjee, M. Elimelech, Langmuir 19 (2003) 4836.
[19] B.H. Lower, R. Yongsunthon, F.P. Vellano, S.K. Lower, J. Bacteriol. 187 (2005) 2127.
[20] P.J. Flory, Statistical Mechanics of Chain Molecules, Hanser Publishers, Munich, 1989.
[21] C. Bustamante, J.F. Marko, E.D. Siggia, S. Smith, Science 265 (1994) 1599.

[22] T.E. Fisher, P.E. Marszalek, A.F. Oberhauser, M. Carrion-Vazquez, J.M. Fernandez, J. Physiol. Lond. 520 (1999) 5.
[23] H. Mueller, H.-J. Butt, E. Bamberg, Biophys. J. 76 (1999) 1072.
[24] R.G. Horn, D.T. Smith, W. Haller, Chem. Phys. Lett. 162 (1989) 404.
[25] G.R. Wiese, R.O. James, T.W. Healy, Discuss Faraday Soc. 52 (1971) 302.
[26] G. Tuin, J. Senders, H.N. Stein, J. Colloid Interface Sci. 179 (1996) 522.
[27] R. Folkersma, A.J.G. van Diemen, H.N. Stein, Langmuir 14 (1998) 5973.
[28] S. Koutsopoulos, J. van der Oost, W. Norde, Langmuir 20 (2004) 6401.
[29] T.N. Murakami, Y. Fukushima, Y. Hirano, Y. Tokuoka, M. Takahashi, N. Kawashima, Colloids Surf. B 29 (2003) 171.